PERIODICO di MINERALOGIA
established in 1930

An International Journal of
MINERALOGY, CRYSTALLOGRAPHY, GEOCHEMISTRY, ORE DEPOSITS, PETROLOGY, VOLCANOLOGY
and applied topics on *Environment, Archaeometry* and *Cultural Heritage*

Geochemistry and palaeoenvironmental significance of Upper Cretaceous clay-rich beds from the Peri-Adriatic Apulia carbonate Platform, southern Italy

FRANCESCO MORELLI[1]*, ROBERT CULLERS[2], ROCCO LAVIANO[1] and GIOVANNI MONGELLI[3]

[1] Dipartimento Geomineralogico, Università di Bari, via E. Orabona, 4 - I-70125 Bari, Italy
[2] Department of Geology, Kansas State University, Thompson Hall, Manhattan, KS, I-66506-3201, USA
[3] Centro di Geodinamica, Università degli Studi della Basilicata, via Anzio, I-85100 Potenza, Italy

Submitted, January 2000 - Accepted, May 2000

ABSTRACT. — Clay-rich beds of Late Cretaceous age (from Cenomanian to Coniacian) interbedded with limestone in the Apulian Carbonate Platform, southern Italy, were analysed for mineralogy, major elements and trace elements. In addition, a number of size fractions of these beds were analysed for mineralogy and chemistry, including REE.

Significant mineralogical and chemical differences were recognized between the beds. The Cenomanian unit is smectite-rich and shows high REE and high strength field element concentrations with a negative Eu/Eu* ratio (0.42), arguing for a fairly felsic source. The role of smectite in controlling most trace elements distribution is minor. The Turonian and Coniacian clay-rich beds are instead illite-rich and have flat REE patterns (normalized to the PAAS), higher Eu/Eu* ratios and lower REE and high strength field element concentrations. The control of illite on most trace elements distribution is also minor.

During the Late Cretaceous the Apulian Carbonate Platform was sheltered from terrigeneous supply by deep troughs. Chemical indicators (i.e. Zr/Ti, $(V+Ni+Cr)/Al_2O_3$, Rb/K_2O), along with the absence of volcanic shards, lithic fragments and diagenetic minerals commonly associated with volcanically-derived clay beds, exclude a volcanic source for the clayey material. It is suggested that the clay-rich beds represent insoluble material, mostly wind-borne derived, from erosion of the exposed carbonate platform and deposited onto submerged portions of the platform itself.

A calcareous breccia bed of Turonian age characterized by a kaolinite-rich reddish matrix was also studied. This bed formed in a warm and humid climate through dissolution of the platform limestone and accumulated on land. It is probably coeval with the karst bauxites of the Apulian Carbonate Platform and its composition has been used to test, in a binary mixing model, the parental relation of the karst bauxite. The (Eu/Eu*) and (Sm/Nd) values support a bauxite derivation from both intermediate composition pyroclastics and limestone residuum according, to the Late Cretaceous palaeotectonic restorations.

RIASSUNTO. — Nel presente lavoro sono state studiate le caratteristiche mineralogiche e chimiche di alcuni livelli pelitici del Cretaceo superiore (dal Cenomaniano al Coniaciano) intercalati nei calcari della Piattaforma carbonatica Apula, Italia meridionale. Inoltre un gruppo di frazioni granulometriche è stato analizzato sotto l'aspetto mineralogico e chimico, incluso il gruppo delle terre rare (REE).

Sono state individuate fra i livelli significative differenze mineralogiche e chimiche. Il livello del

* Corresponding author, E-mail: f.morelli@geomin.uniba.it
rocco.laviano@geomin.uniba.it
rcullers@ksu.edu
mongelli@unibas.it

Cenomaniano è ricco in smectite e mostra alte concentrazioni di REE e di elementi ad alta forza di campo assieme ad un rapporto Eu/Eu* negativo, indicativi di una sorgente abbastanza felsica. Il ruolo della smectite nel controllo della distribuzione degli elementi in traccia è minore. I livelli argillosi del Turoniano e del Coniaciano sono invece ricchi in illite ed hanno un pattern delle terre rare piatto (normalizzato alle PAAS), rapporti Eu/Eu* più alti e concentrazioni più basse di REE ed elementi ad alta forza di campo. Il controllo dell'illite nella distribuzione della maggior parte degli elementi in traccia è minore.

Nel Cretaceo superiore la Piattaforma carbonatica Apula era protetta da apporti terrigeni attraverso profonde depressioni. Gli indicatori chimici (per esempio Zr/Ti, (V+Ni+Cr)/Al_2O_3, Rb/K_2O) assieme all'assenza di frammenti vulcanici, frammenti litici e minerali diagenetici comunemente associati a livelli argillosi derivati da materiale vulcanico, escludono una origine vulcanica per questo livello argilloso.

Si sostiene che i livelli pelitici rappresentino il materiale insolubile, principalmente derivato da trasporto eolico, proveniente dall'erosione della piattaforma carbonatica esposta e depositatosi su porzioni sommerse della piattaforma stessa.

È stato inoltre studiato un livello di breccia calcarea del Turoniano caratterizzato da una matrice rossastra ricca in caolinite. Questo livello si è formato in un clima caldo e umido attraverso la dissoluzione del calcare di piattaforma e si è accumulato sul terreno. È probabile che esso sia coevo alle bauxiti carsiche della Piattaforma carbonatica Apula e la sua composizione è stata usata per verificare, in un modello di mescolamento binario, la relazione parentale con la bauxite carsica. I valori di Eu/Eu* e Sm/Nd confermano una bauxite di derivazione sia da materiale piroclastico di composizione intermedia sia dal residuo insolubile del calcare, in accordo con le ricostruzioni paleotettoniche del Cretaceo superiore.

KEY WORDS: *Clay-rich beds, geochemistry, carbonate platfom, wind-borne dust, bauxite.*

INTRODUCTION

The stratigraphy of the Italian Peninsula successions reflects the geodynamic evolution of the central Mediterranean, and the Late Permian to Cretaceous sequences record the history of the Tethys margin (Doglioni and Flores, 1994). During that time, the Italian Peninsula was part of the passive margin of the Western and Northern Adria microplate during the opening of the Western Tethys oceanic basin. In the Early Jurassic, due to crustal extension, many shallow water sediments were submerged and only some isolated carbonate platforms (the Peri-Adriatic Platforms) persisted, sheltered from terrigenous influx by deep troughs. Some of these carbonate shelf areas, like the Apulia Carbonate Platform (ACP), situated along the southern margin of the Tethys ocean, persisted throughout the Cretaceous. In the Late Cretaceous (fig. 1), most of the Peri-Adriatic Platforms underwent exposure, in contrast with the worldwide retreat of carbonate platforms during that time (Schlanger, 1981). Platform exposure clashed with tectonic rearrangement, from extensional to compressional, of part of the Tethyan realm (Eberli, 1991). As a consequence, the Adria plate came into collision with Europe, and the Peri-Adriatic Platforms were included into the foldbelts of the Alpine-Mediterranean Chain.

The carbonate sequence records the evolution of the palaeogeographic settings by changes in its sedimentological, chemical and isotopic features (e.g., Jenkyns, 1988, 1995; Ferreri *et al.*, 1997; Carannante *et al.*, 1997). In some Peri-Adriatic Platforms, clay-rich beds are often found, and the geochemistry and mineralogy of these layers may provide additional constraints on the formation of carbonate platforms. As no chemical or mineralogical studies exist on the pelitic beds of the Late Cretaceous of the ACP, the present work was undertaken to provide compositional features of these beds, in order to assess palaeoenvironmental changes in the ACP.

GEOLOGICAL SETTINGS

The ACP is mostly composed of a Mesozoic carbonate succession. Its outcrops are mainly Cretaceous and consist almost entirely of inner platform limestone, which changes to a slope facies in the Campanian (Luperto Sinni, 1996). The succession is divided into two parts by an angular unconformity, which is Turonian in age and is marked by either clay or bauxite accumulation (Iannone and Laviano, 1980;

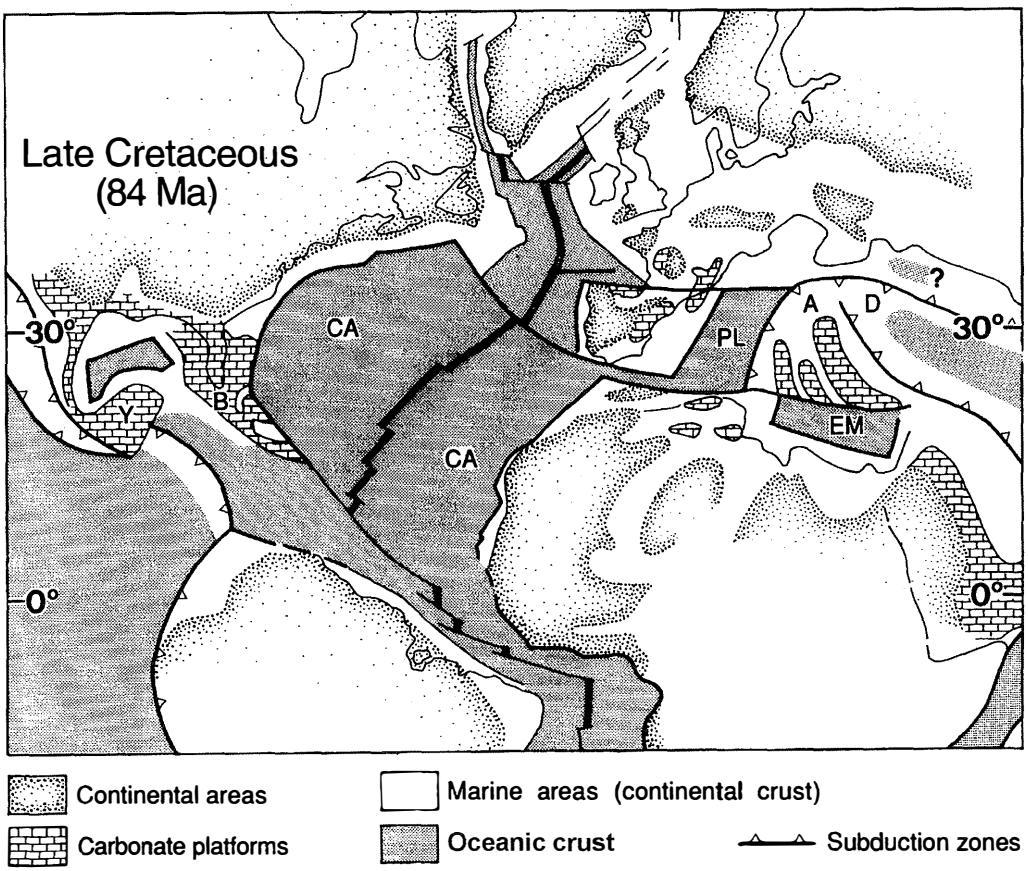

Fig. 1 – Late Cretaceous palaeogeography within framework of Cretaceous Tethys ocean. A: Apulia Carbonate Platform; EM: Eastern Mediterranean; PL: Piemonte-Liguria Ocean; CA: Central Atlantic (from Eberli *et al.*, 1993, modified).

Luperto Sinni and Reina, 1996; Laviano *et al.*, 1998). The lower part of the succession is represented by the «Calcare di Bari» Formation, which is composed of micritic and biomicritic limestone, bioclastic limestone, calcirudite and calcarenite. In the Upper Cenomanian-Lower Turonian, the depositional environment evolved from a shelf-lagoon low energy system to a tractive current high energy system, and then again to a low energy environment followed by emergence of the platform. The deposition of the upper part of the succession, the micritic «Calcare di Altamura» Formation, started during the Senonian in shallow water (Iannone and Laviano, 1980). Further depositional gaps during the Late Cretaceous are documented in the western area of the ACP (e.g. Luperto Sinni, 1996).

Sampling and analytical procedures

The studied pelitic samples derive from different stratigraphic levels (fig. 2):

1) Samples AC1 and AC2 were collected from a bed in the Cenomanian (Iannone and Laviano, 1980; Luperto Sinni, 1996) of the «Calcare di Bari» Formation.

2) Samples BR1 and BR2 come from a breccia layer formed of calcareous clasts embedded in a reddish pelitomorphic matrix.

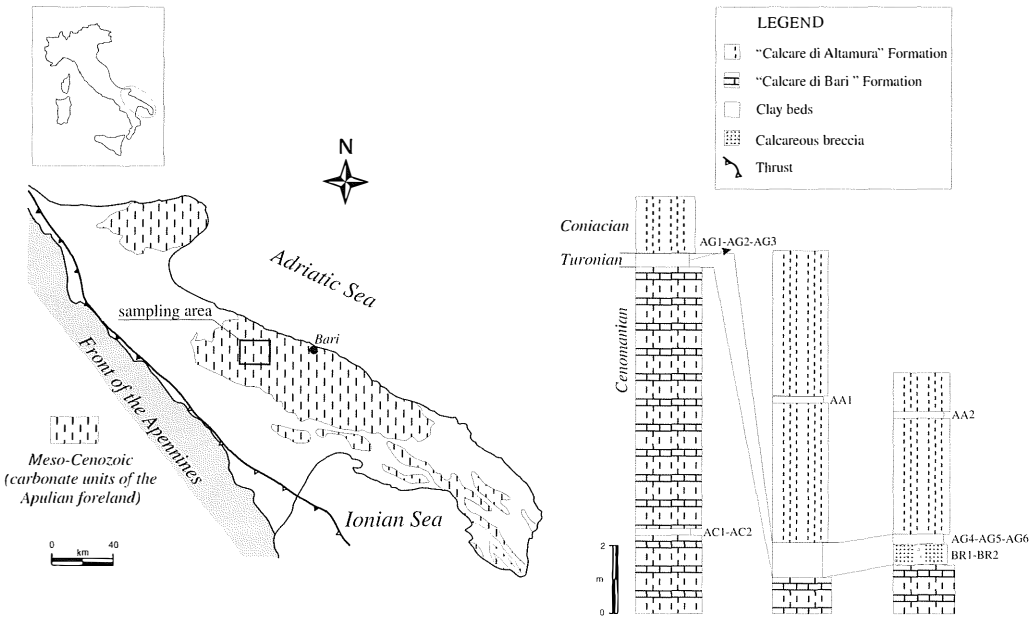

Fig. 2 – Geological sketch map of Apulian area and simplified stratigraphic section of sampling sites and location of pelitic beds.

The clasts were deposited on to the erosion surface which developed at the top of the «Calcare di Bari» Formation. The age of deposition is related to the Turonian emergence stage of the ACP (Luperto Sinni, 1996).

3) Samples AG 1 to 6 derive from the clay-rich bed recognized by Iannone and Laviano (1980) and associated with the Turonian hiatus. Three of these samples were collected from a level overlapping the breccia layer.

4) Samples AA1 and AA2 refer to a bed in the Coniacian of the «Calcare di Altamura» Formation (Luperto Sinni, 1996).

Gravity settling in deionized water was used to separate grain-size fractions <2 μm, 2-64 μm, and >64 mm from samples. Only the reddish pelitomorphic matrix from the breccia samples was separated by wet sieving (<500 μm). Samples AC1, BR1, AG5 and AA1 were separated into additional grain-size fractions of 2-4, 4-8, 8-16, 16-32 and 32-64 μm in order to perform chemical mass balance calculations (e.g., Mongelli *et al.*, 1996). To obtain all the material of each fraction, at least five decantation cycles were carried out. Mineralogy of whole rocks and grain-size fractions was determined by XRD (CuK_α, Ni filtered radiation) according to Laviano (1987). The illite crystallinity index (Weber *et al.*, 1976) and the smectite crystallinity index (Biscaye, 1965) were determined in the <2 μm size fractions after glycol solvation.

In whole rocks and <2 μm grain-size fractions, the contents of major elements, Rb, Ba, Sr, V, Cr, Ni, Y, Zr and Nb were obtained by XRF methods, as described in Franzini *et al.* (1972, 1975) and Leoni and Saitta (1976), with a precision for major elements better than 10%. In selected whole rocks AC1, BR1, AG5 and AA1 and separated grain-size fractions, Rb, Ba, Th, Hf, Ta, Co, Sc, Cr, Cs, La, Ce, Sm, Eu, Tb, Yb and Lu contents were determined by neutron activation according to Gordon *et al.* (1968) and Jacobs *et al.* (1977). The analytical precision for trace elements was better than 5%, except for Yb and Lu (7%).

TABLE 1

Grain-size distribution in bulk rocks (weight %), and classification according to Shepard (1954).

Sample	CLAY (<2 μm)	SILT (2-64 μm)	SAND (>64 μm)
AA1	35.92	31.83	32.25
AA2	23.66	40.3	36.04
AG1	20.73	45.83	33.44
AG2	30.4	55.01	14.59
AG3	24.44	41.46	34.1
AG4	30.63	57.41	1 1.96
AG5	25.34	28.29	46.37
AG6	28.42	47.25	24.33
BR1	73.96	25.15	0.89
BR2	58.72	26.36	14.92
AC1	75.05	2 1.87	3.08
AC2	80.92	18.95	0.13

RESULTS

Grain size distribution and mineralogy

The grain-size distribution (Table 1) shows that the oldest samples only, i.e. samples AC1 and AC2 from the Cenomanian of the «Calcare di Bari» Formation, are mostly clay (<2 μm grain-size fraction ≥75% by weight). The matrix of the BR samples is composed of silty-clay, whereas the AG and AA samples are composed of significant amounts of silt and sand, and may be classified as sand-silt-clay and clayey silt. From the more detailed grain-size distribution reported in Table 2, the main granulometric difference among of pelitic layers is the amount of sand, with low values in AC1 and BR1 and high values in AG5 and AA1. In the latter rocks, sand greatly dilutes the clay-silt fraction.

TABLE 2

Detailed grain-size distribution (weight %) in selected samples.

Sample	<2 μm	2-4 μm	4-8 μm	8-16 μm	16-32 μm	32-64 μm	>64 μm
AA1	35.92	11.28	7.94	7.78	3.83	1.00	32.25
AG5	25.34	8.45	7.85	5.87	4.65	1.47	46.37
BR1	73.96	7.73	6.64	4.87	5.49	0.42	0.89
AC1	75.05	6.93	7.06	5.50	2.28	0.10	3.08

TABLE 3

Mineralogical composition (weight %) of bulk rocks. n.d. = not detected; tr = trace; Ill = illite; Ms = muscovite.

Sample	Smectite	Ill+Ms	Kaolinite	Chlorite	Goethite	Quartz	Feldspars	Calcite	Dolomite	Clay min.
AA1	6	31	tr	2	tr	3	1	57	tr	39
AA2	17	20	4	5	n.d.	7	3	44	tr	46
AG1	16	20	1	3	tr	6	1	53	tr	40
AG2	15	21	tr	2	tr	3	1	58	tr	38
AG3	8	30	tr	2	tr	5	2	53	tr	40
AG4	12	27	1	tr	n.d.	3	2	55	tr	40
AG5	3	21	tr	2	n.d.	5	3	66	tr	26
AG6	7	29	tr	tr	n.d.	4	2	58	tr	36
BR1	7	18	58	4	7	4	1	1	tr	87
BR2	8	19	39	6	4	8	2	14	tr	72
AC1	58	6	19	8	n.d.	3	2	4	tr	91
AC2	65	9	15	5	n.d.	3	2	1	tr	94

TABLE 4

Mineralogical distribution (weight %) in grain-size fractions. n.d. = not detected; tr = trace.

<2 µm

Sample	Smectite	Illite	Kaolinite	Chlorite	Goethite	Quartz	Feldspars	Calcite	Dolomite	Clay min.
AA1	12	64	tr	3	tr	2	tr	19	tr	79
AA2	46	36	4	2	n.d.	3	1	8	n.d.	88
AG1	43	40	2	tr	tr	4	1	10	tr	85
AG2	40	49	tr	tr	tr	2	1	8	tr	89
AG3	15	68	tr	tr	tr	3	tr	14	tr	83
AG4	21	45	3	tr	n.d.	3	2	26	n.d.	69
AG5	6	54	-	tr	n.d.	3	2	35	n.d.	60
AG6	12	56	tr	tr	n.d.	3	1	28	n.d.	68
BR1	8	21	61	tr	3	4	2	1	n.d.	90
BR2	10	25	55	tr	2	6	1	1	n.d.	90
AC1	65	6	18	6	n.d.	3	2	tr	tr	95
AC2	70	8	16	4	n.d.	2	tr	tr	n.d.	98

2-64 µm

Sample	Smectite	Illite	Kaolinite	Chlorite	Goethite	Quartz	Feldspars	Calcite	Dolomite	Clay min.
AA1	5	22	n.d.	4	n.d.	2	tr	67	tr	31
AA2	15	24	7	9	n.d.	11	5	29	n.d.	55
AG1	17	22	tr	3	n.d.	8	3	47	n.d.	42
AG2	5	11	tr	3	n.d.	3	tr	77	1	19
AG3	10	30	tr	4	n.d.	8	2	46	tr	44
AG4	9	22	tr	tr	n.d.	3	2	64	tr	31
AG5	3	18	tr	2	n.d.	3	tr	74	n.d.	23
AG6	7	26	tr	tr	n.d.	5	2	60	tr	33
BR1	5	11	49	16	12	5	1	1	n.d.	81
BR2	8	11	26	18	6	8	4	19	tr	63
AC1	44	8	25	14	tr	4	2	3	n.d.	91
AC2	43	10	14	10	n.d.	9	10	3	1	77

> 64 µm

Sample	Illite	Chlorite	Goethite	Quartz	Feldspars	Calcite	Dolomite
AA1	3	n.d.	n.d.	3	3	91	n.d.
AA2	5	2	n.d.	5	2	86	n.d.
AG1	3	5	n.d.	4	tr	88	n.d.
AG2	2	tr	n.d.	5	2	91	n.d.
AG3	4	2	n.d.	3	2	89	n.d.
AG4	3	2	n.d.	4	3	88	n.d.
AG5	5	3	n.d.	8	6	78	n.d.
AG6	3	2	n.d.	4	2	89	tr
BR1	7	8	41	12	8	24	n.d.
BR2	6	3	16	14	4	57	n.d.
AC1	1	3	n.d.	3	3	90	n.d.
AC2	6	5	n.d.	5	4	80	n.d.

Mineralogy of bulk samples consists of illite, smectite, chlorite, kaolinite, quartz, calcite and feldspars (Table 3), but the relative proportions of minerals changes significantly in different beds. The enrichment order of minerals in AC samples is: smectite >> kaolinite > illite ≈ chlorite > quartz ≈ feldspars ≈ calcite. In BR samples: kaolinite >> illite > smectite > goethite ≈ chlorite ≈ quartz > feldspars ≈ calcite; goethite is also present in appreciable amounts in the sand fraction of the matrix. In AG and AA samples, calcite predominates, i.e.: calcite >> illite > smectite > quartz > chlorite ≈ feldspars > kaolinite. In all samples, calcite is concentrated in the sand fraction, and illite, smectite and kaolinite in the clay fraction (Tables 4 and 5).

Calcite in the sand fractions is reworked, whereas in the finest fractions it appears to be authigenic. Smectite is dioctahedral ((060) ≈ 1.50 Å); Ca-Mg ((001) ≈ 14.0 Å) and has a montmorillonite compositional affinity. Its crystallinity index ranges from medium to high (Table 6). The highest *v/p* index values refer to smectite from AC samples, the mineral being better ordered than in the other samples. Illite is dioctahedral and generally has a low crystallinity index (Table 6). The amount of expandable layers ranges from 0% to 15% (Srodon, 1980). Feldspars are generally weathered plagioclase and orthoclase.

Chemistry

Chemical data of bulk rocks are given in Table 7, and chemical composition of fractions in selected samples in Table 8. Data normalized to the Upper Continental Crust (UCC, Taylor and McLennan, 1985) for selected samples are compared in fig. 3. AG and AA samples have whole rock CaO_{sample}/CaO_{UCC} ratios of ≈ 10, whereas BR and AC samples have CaO contents well below the UCC average. BR rocks are enriched in Fe_2O_3, Sc, V, Cr, Ni, Th and REE relative to UCC; AC rocks have Fe_2O_3, Sc and Ni contents comparable with those of carbonate-rich rocks, but are depleted in Co and enriched in Th, V and Cr relative to UCC.

The main features of trace element percent contribution of grain-size fractions in selected rocks (concentration densities are given in fig. 4) are: in samples AC1 and BR1, the lowest concentration densities are usually observed in the <2 μm grain-size fraction where smectite and kaolinite, respectively, are the most

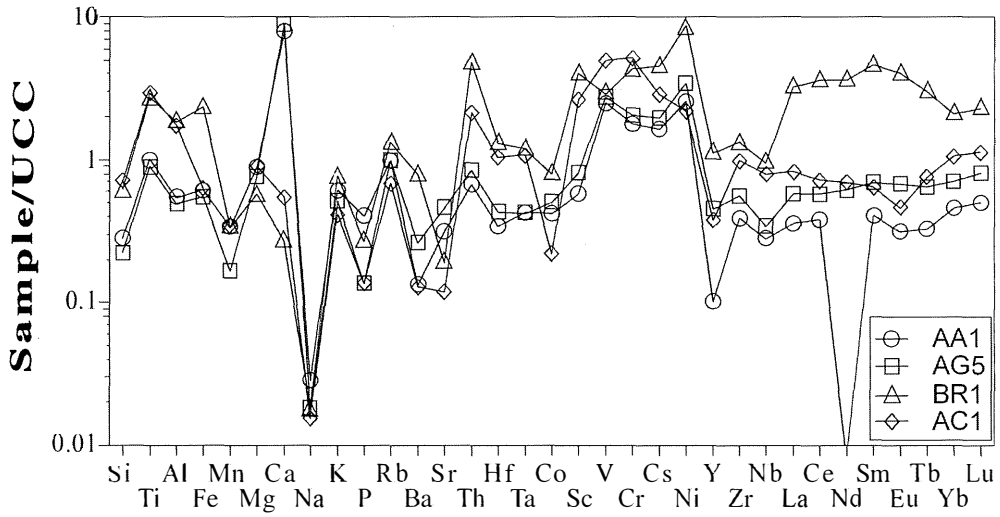

Fig. 3 – Major and trace elements composition of selected samples normalized to Upper Continental Crust (UCC, Taylor and McLennan, 1985). See text.

TABLE 5

Mineralogical distribution (weight %) in detailed grain-size fractions of selected samples.

AA1	Smectite	Illite	Kaolinite	Chlorite	Goethite	Quartz	Feldspars	Calcite	Dolomite	Clay min.
<2 μm	12	64	tr	3	n.d.	2	tr	19	tr	79
2-4 μm	9	34	n.d.	5	n.d.	2	tr	50	n.d.	48
4-8 μm	4	21	n.d.	4	n.d.	2	tr	69	n.d.	29
8-16 μm	4	16	n.d.	2	n.d.	2	tr	76	n.d.	22
16-32 μm	n.d.	10	n.d.	4	n.d.	2	tr	84	n.d.	14
32-64 μm	n.d.	3	n.d.	1	n.d.	2	tr	94	n.d.	4
>64 μm	n.d.	3	n.d.	n.d.	n.d.	3	3	91	n.d.	3
AG5										
<2 μm	6	54	n.d.	tr	n.d.	3	2	35	n.d.	60
2-4 μm	5	18	n.d.	tr	n.d.	2	1	74	n.d.	23
4-8 μm	4	19	n.d.	2	n.d.	3	tr	72	n.d.	25
8-16 μm	2	21	n.d.	2	n.d.	3	tr	72	n.d.	25
16-32 μm	n.d.	12	n.d.	5	n.d.	4	tr	79	n.d.	17
32-64 μm	n.d.	7	n.d.	2	n.d.	3	tr	88	n.d.	9
>64 μm	n.d.	5	n.d.	3	n.d.	8	6	78	n.d.	8
BR1										
<2 μm	8	21	61	tr	3	4	2	1	n.d.	90
2-4 μm	6	12	53	18	8	3	tr	tr	n.d.	89
4-8 μm	8	10	55	12	11	3	tr	1	n.d.	85
8-16 μm	6	12	45	17	13	6	tr	1	n.d.	80
16-32 μm	n.d.	10	42	20	15	8	2	3	n.d.	72
32-64 μm	n.d.	18	n.d.	9	42	10	5	16	n.d.	27
>64 μm	n.d.	7	n.d.	8	41	12	8	24	n.d.	15
AC1										
<2 μm	65	6	18	6	n.d.	3	2	tr	tr	95
2-4 μm	56	6	16	12	n.d.	4	3	3	n.d.	90
4-8 μm	49	8	25	14	tr	2	1	1	n.d.	96
8-16 μm	42	10	20	19	tr	4	2	3	n.d.	91
16-32 μm	tr	4	64	12	tr	11	1	8	n.d.	80
32-64 μm	n.d.	10	22	33	tr	15	2	18	n.d.	65
>64 μm	n.d.	1	n.d.	3	n.d.	3	3	90	n.d.	4

n.d. = not detected; tr = trace.

TABLE 6

Calculated crystallinity indexes of illite and smectite in <2 μm size fraction. n.d. = not detected.

Sample	**Smectite**	**Illite**	Sample	**Smectite**	**Illite**
AA1	n.d.	115	**AG5**	n.d.	70
AA2	0.65	45	**AG6**	n.d.	87
AG1	0.51	80	**BR1**	n.d.	100
AG2	0.59	76	**BR2**	0.54	40
AG3	0.74	80	**AC1**	0.75	n.d.
AG4	n.d.	57	**AC2**	0.96	n.d.

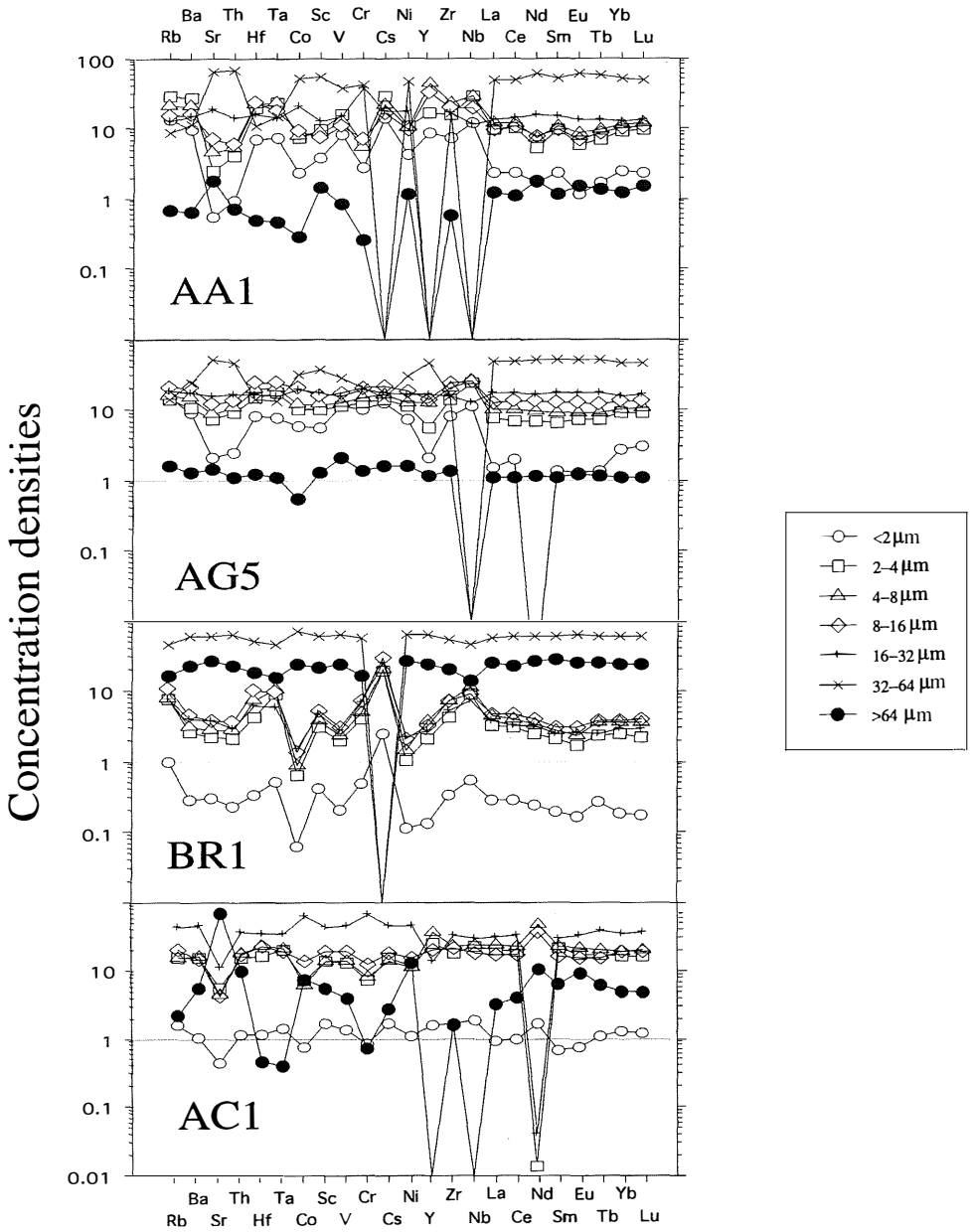

Fig. 4 – Grain-size fraction contribution to whole rock (in selected samples) as trace element concentration densities.

abundant. Sample AC1 has the highest concentration densities in the 16-32 µm grain-size fraction. An exception is represented by Sr, which concentrates in the sand fraction, probably due to the abundance of calcite Sr being a possible substitute of Ca in $CaCO_3$. The contribution of the 4-8 µm grain-size fraction, mineralogically composed of

TABLE 7

Chemical composition of bulk rocks. n.d. = not detected. C.I.A. = alteration chemical index.

Sample	AC1	AC2	BR1	BR2	AG1	AG2	AG3	AG4	AG5	AG6	AA1	AA2
wt%												
SiO_2	46.00	47.70	40.5	35.6	20.9	18.90	20.80	20.10	14.80	17.50	18.50	25.30
TiO_2	1.48	1.40	1.38	1.33	0.50	0.47	0.60	0.49	0.45	0.42	0.51	0.74
Al_2O_3	26.40	25.80	27.6	25.50	10.10	8.9	10.30	9.46	7.51	8.44	8.09	14.30
Fe_2O_3	3.10	2.98	11.6	7.26	3.23	2.7	3.12	3.66	2.71	2.53	3.06	2.29
MnO	n.d.	n.d.	0.02	0.02	0.03	0.02	0.03	0.02	0.01	0.02	0.02	0.01
MgO	1.98	2.26	1.26	0.94	1.80	1.70	1.81	2.05	1.68	1.97	1.95	1.66
CaO	2.33	1.54	1.15	8.38	30.80	33.30	30.00	31.00	37.90	33.50	33.40	25.80
Na_2O	0.06	0.05	0.07	0.05	0.07	0.07	0.08	0.09	0.07	0.1	0.11	0.08
K_2O	1.43	1.38	2.61	1.97	2.16	1.86	2.45	2.42	1.75	2.04	2.11	2.32
P_2O_5	0.01	0.01	0.02	0.01	0.05	0.05	0.04	0.02	0.01	0.02	0.03	0.01
LOI	17.21	17.00	13.79	18.95	30.36	32.03	30.77	30.69	33.11	33.46	32.22	27.49
ppm												
Rb	78	63	150	118	103	92	111	100	112	82	112	94
Ba	71	69	440	247	202	165	238	140	144	129	73	215
Sr	42	41	67	53	103	66	121	130	160	138	110	89
Th	23		52						9		7	
Hf	6		8						3		2	
Ta	2	n.d.	3			n.d.			1	n.d.	1	n.d.
Co	2		8						5		4	
Sc	29		45						9		6	
V	299	453	172	132	123	100	74	123	164	79	149	91
Cr	183	184	151	205	51	49	53	60	71	52	63	82
Cs	11		17						7		6	
Ni	44	39	176	158	45	37	47	73	69	48	51	67
Y	8	9	25	12	12	3	8	13	10	10	2	5
Zr	187	201	255	201	86	74	93	85	108	70	75	112
Nb	20	21	24	22	7	6	9	6	9	5	7	10
La	25	27	96	24	33	13	23	48	17	21	11	18
Ce	46	44	230	40	50	17	46	66	37	43	24	34
Nd	18		93						16		n.d.	
Sm	3		21						3		2	
Eu	0.4	n.d.	3.5			n.d.			0.6	n.d.	0.3	n.d.
Tb	0.5		2						0.4		0.2	
Yb	2.3		5						1.6		1	
Lu	0.4		0.7						0.3		0.2	
Σ REE	95.6	451.2						75.9		38.7		
C.I.A.	94	91	-	-	75	76	78	78	73	73	69	80
Th/Co10.4	-	6.53	-	-	-	-	-	1.8	-	1.74	-	
Eu/Eu*	0.417	-	0.619	-	-	-	-	-	0.615	-	0.551	-
SiO_2/Fe_2O_3+ +MgO	9.051	9.105	3.139	4.344	4.155	4.298	4.211	3.535	3.367	3.891	3.687	6.418

smectite+kaolinite, is important for some high field strength elements (HFSE), i.e. Th, Hf, Ta, Zr and Nb and REE. The highest concentration densities are observed in the 32-64 mm grain-size fraction of sample BR1 and, subordinately, in the sand fraction. Goethite is the main mineral in both these grain-size fractions.

The lowest concentration densities are usually observed in the >64 mm grain-size fraction of samples AG5 and AA1, where calcite dominates and, to a lesser extent, in the <2 mm grain-size fraction, where illite dominates. In both samples the highest concentration densities are usually associated with the silt fraction and particularly in coarser silt (32-64 μm), where calcite again concentrates.

Discussion

Smectite-rich bed (samples AC)

The occurrence of smectite in a marine setting is generally related to the transformation of volcanic ash, but smectites in the marine sediments do not systematically and easily form in the marine environment, and do not automatically result from the alteration of volcanic rocks (Chamley, 1989). The distribution of REE, HFSE and first row transition elements, together with the mineralogical characterization of smectite, is an important approach to investigate the origin of smectite-rich marine sediments (Wray, 1995; Andreozzi *et al.*, 1997; Laviano and Mongelli, 1996). Wray (1995) showed that smectite from alteration of volcanics in Cretaceous beds exhibits REE patterns with negative Eu-anomaly and HREE depletion relative to the average shale. Instead, coeval detrital clays display flat patterns. Similarly, Laviano and Mongelli (1996) observed that bentonitic clays of Oligo-Miocene age have negative Eu-anomalies with respect to the PAAS. Andreozzi *et al.* (1997) used Zr/Ti and $(V+Cr+Ni)/Al_2O_3$ values to discriminate between volcaniclastic and «normal» terrigeneous marine sediments. The Zr/Ti ratio is considered to be a genetic indicator, whereas the $(V+Cr+Ni)/Al_2O_3$ ratio should be indicative of diagenetic modifications, as transition elements are sensitive to redox changes, degradation or transformation of organic matter and phyllosilicate recrystallization. In the Zr/Ti vs $(V+Cr+Ni)/Al_2O_3$ plot, the smectite-rich samples from the current study fall in the field of terrigeneous sediments (fig. 5*a*). Similarly, the Rb *vs* K_2O plot (fig. 5*b*; Planck and Langmuir, 1998) also excludes the volcanoclastic origin of precursors of the smectite-rich beds of the ACP. This

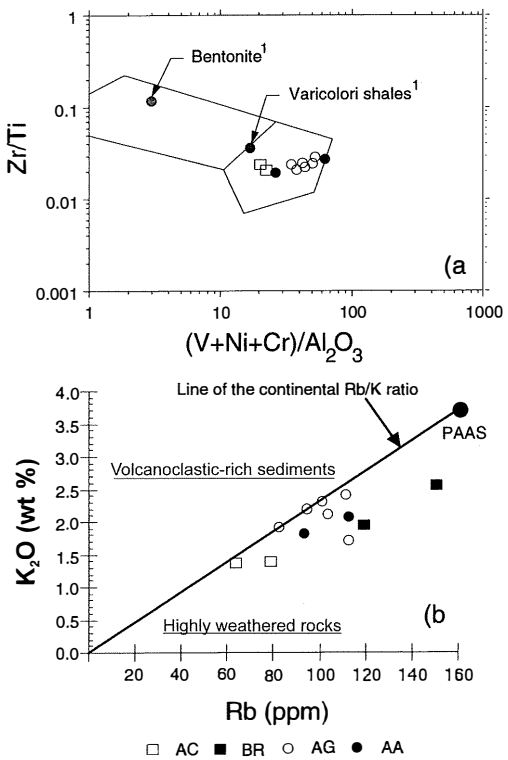

Fig. 5 – *a)* Plot discriminating transformed volcaniclastic sediments (left) and «normal» terrigeneous sediments (right), after Andreozzi *et al.* (1997). The diagram correctly discriminates between volcanic-derived (bentonite) and terrigeneous shales «vari colori» of Cenozoic age from southern Apennines (Laviano and Mongelli, 1996). *b)* Low K/Rb ratio is typical of ancient and highly weathered rocks; high K/Rb ratio is typical of sediments rich in volcanoclastics (Planck and Langmuir, 1998).

TABLE 8

Chemical composition of grain-size fractions in selected samples. n.d. = not detected.

BR 1	<2 μm	2-4 μm	4-8 μm	8-16 μm	16-32 μm	32-64 μm	>64 μm
wt%							
SiO_2	40.60	39.30	37.40	36.90	34.80	15.00	13.30
TiO_2	1.34	2.58	2.51	1.63	1.30	0.82	0.61
Al_2O_3	27.80	28.80	27.80	27.00	25.36	10.70	9.45
Fe_2O_3	9.94	11.20	13.90	14.6	17.00	43.60	40.50
MnO	0.02	0.02	0.02	0.02	0.02	0.06	0.06
MgO	1.10	0.79	0.78	0.89	0.93	0.73	0.58
CaO	1.45	0.71	0.93	1.50	2.57	9.12	14.00
Na_2O	0.07	0.08	0.07	0.05	0.05	0.05	0.06
K_2O	2.54	1.95	1.82	1.96	1.97	1.10	0.83
P_2O_5	0.02	0.02	0.03	0.02	0.02	0.03	0.02
LOI	15.12	14.55	14.74	15.43	15.98	18.79	20.59
ppm							
Rb	164	133	118	119	97	45	33
Ba	375	356	369	397	384	453	361
Sr	62	49	52	51	59	69	66
Th	41	38	44	41	38	64	48
Hf	5	6	10	9	7	4	3
Ta	3	5	5	3	2	1	1
Co	8	8.0	10	11	14	48	35
Sc	38	30	31.0	32.0	31	30	24
V	127	126	127	127	129	225	175
Cr	168	141	152	162	170	111	68
Cs	17	14	13	14	13	n.d.	n.d.
Ni	177	177	208	224	267	591	511
Y	19	32	49	31	30	51	40
Zr	228	306	438	322	262	207	172
Nb	23	40	43	26	23	11	7
La	69	83	98	76	70	81	74
Ce	150	169	186	162	124	180	148
Nd	74	78	92.0	79	72	103	97
Sm	16	18	21	17	15	29	29
Eu	3	3	3	3	3	6	5
Tb	2	2	2	2	1	3	2
Yb	4	5	6	5	4	7	6
Lu	0.6	0.7	1	1	1	1	1
ΣREE	318.6	358.7	409	345	290	410	362

interpretation is consistent with the lack of both volcanic shards and lithic fragments, as well as zeolites commonly associated with volcanically-derived smectite horizons. Instead, the REE patterns of sample AC1, when normalized to PAAS, are not flat as expected and have $(La/Yb)_{PAAS}$=0.79 and a negative Eu-anomaly (Eu/Eu*=0.66) relative to the PAAS (fig. 6). The REE signature of volcanically-derived smectitic beds mainly reflects the original composition as modified by diagenetic changes in the marine environment (e.g., see Wray, 1995). The REE patterns of seawater, normalized to shales, have a large negative Ce-anomaly coupled with a lack of Eu-anomaly (e.g., Zhang and Nozaki, 1998) and authigenic

TABLE 8. *continued*

AA1	<2 μm	2-4 μm	4-8 μm	8-16 μm	16-32 μm	32-64 μm	>64 μm
wt%							
SiO_2	38.30	22.50	12.90	9.29	4.78	0.96	2.42
TiO_2	0.90	0.86	0.69	0.45	0.21	0.04	0.06
Al_2O_3	16.50	10.10	6.13	4.29	2.21	0.54	1.11
Fe_2O_3	6.22	3.80	2.33	1.95	1.67	1.34	0.88
MnO	0.01	0.02	0.02	0.02	0.02	0.02	0.02
MgO	3.51	2.24	1.45	1.21	0.92	0.69	0.94
CaO	11.10	28.70	39.50	43.8	48.60	53.10	51.70
Na_2O	0.15	0.19	0.12	0.11	0.14	0.14	0.12
K_2O	4.30	2.70	1.52	1.04	0.52	0.10	0.26
P_2O_5	0.02	0.02	0.04	0.04	0.10	0.10	0.10
LOI	18.99	28.87	35.3	37.8	40.83	42.97	42.39
ppm							
Rb	220	147	76	55	22	4	10
Ba	183	160	89	66	31	6	11
Sr	63	92	115	175	226	205	181
Th	8	11	11	11	14	17	6
Hf	3	3	2	2	1	n.d.	n.d.
Ta	2	2	1	1	n.d.	n.d.	n.d.
Co	6	6	4	5	5	3	1
Sc	11	9	5	5	4	4	4
V	327	191	113	91	62	40	30
Cr	103	69	44	56	151	43	9
Cs	13	8	5	3	2	n.d.	n.d.
Ni	92	71	49	45	39	28	22
Y	5	3	5	4	n.d.	n.d.	n.d.
Zr	147	101	101	88	36	9	11
Nb	17	13	9	6	2	n.d.	n.d.
La	14	18	16	13	9	8	6
Ce	30	40	34.0	29	19	17	12
Nd	n.d.	n.d.	n.d	n.d.	n.d.	n.d.	n.d
Sm	3	4	3	3	2	2	1
Eu	0.2	0.3	0.4	0.3	0.3	0.4	0.3
Tb	0.3	0.3	0.3	0.3	0.2	0.2	0.2
Yb	1	1	1	1	1	1	1
Lu	0.2	0.2	0.2	0.2	0.1	0.1	0.1
ΣREE	48.7	63.8	54.9	46.8	31.6	28.7	20.6

marine sediments have a peculiar negative Ce-anomaly (e.g., Bonnot-Courtois, 1981). This indicates that smectite formation did not occur in equilibrium with seawater and that the REE patterns of sample AC1 probably reflect the original composition of the parent. This is also consistent with the mass balance of this sample, indicating the importance of smectite in controlling REE, which are probably hosted by primary accessory minerals in the silt fraction.

In the Tethyan realm, both the Upper Cretaceous compressional regime (Eberli, 1991) and the seaward change of the coastal onlap observed in the Cenomanian (Haq *et al.*, 1988) may have promoted the emergence of a shallow-water platform wich, in turn, favoured the formation of a smectite-rich carbonate

TABLE 8. *continued*

AC1	<2 μm	2-4 μm	4-8 μm	8-16 μm	16-32 μm	>64 μm
wt%						
SiO_2	47.30	44.50	45.40	45.10	41.60	1.53
TiO_2	1.47	1.76	1.83	1.34	1.24	0.04
Al_2O_3	26.60	27.10	27.10	25.60	23.70	0.84
Fe_2O_3	3.13	2.78	3.07	3.41	3.93	1.67
MnO	n.d	n.d	n.d	n.d	n.d	n.d
MgO	2.03	1.68	1.72	1.89	1.86	0.50
CaO	0.96	2.53	1.88	2.66	5.80	52.8
Na_2O	0.09	0.10	0.06	0.05	0.05	0.11
K_2O	1.51	1.29	1.26	1.32	1.33	0.06
P_2O_5	0.01	0.02	0.01	0.01	0.01	0.10
LOI	16.9	18.24	17.67	18.62	20.48	42.35
ppm						
Rb	89	79	80	82	75	5
Ba	76	104	112	78	101	17
Sr	37	44	35	26	29	248
Th	23	29	34	25	22	8
Hf	6	8	11	9	6	n.d
Ta	3	3	4	3	2	n.d
Co	2	2	2	3	5	1
Sc	34	25	25	28	26	5
V	293	269	293	309	308	37
Cr	196	158	175	214	492	7
Cs	12	10	10	10	10	1
Ni	47	47	46	49	59	23
Y	10	15	22	10	3	n.d
Zr	211	215	280	197	126	8
Nb	22	25	27	16	11	n.d
La	23	46	54	31	24	3
Ce	45	82	97	58	46	7
Nd	14	n.d.	37	22	n.d.	4
Sm	2	6	7	4	3	1
Eu	0.4	1	1	0.6	0.5	0.2
Tb	0.4	0.6	1	n.d.	0.5	0.1
Yb	3	3	4	3	2	0.4
Lu	0.4	0.4	0.6	0.4	0.3	0.1
ΣREE	88.2	139	201.6	119	76.3	15.8

residuum (cfr. Chamley, 1989), later accumulating as beds on to submerged portions of the platform.

Kaolinite+goethite-rich bed (samples BR) and its relationships with coeval Apulian karst bauxites

Field evidence and mineralogical assemblages indicate that these samples formed in a continental environment through dissolution of platform carbonates in a warm, humid climate. The climate in the Cretaceous was warm and subtropical (Price, 1999), promoting the formation of bauxite deposits as in the case of the Turonian karst bauxites of the ACP (e.g., D'Argenio *et al.*, 1986). The Apulian bauxites are composed of Al-hematite, boehmite,

TABLE 8, *continued*

AG 5	<2 μm	2-4 μm	4-8 μm	8-16 μm	16-32 μm	32-64 μm	>64 μm
wt%							
SiO_2	29.70	10.30	10.30	10.40	7.35	2.67	7.58
TiO_2	0.63	0.48	0.51	0.42	0.22	0.07	0.19
Al_2O_3	14.10	5.10	5.24	5.20	3.61	1.35	3.63
Fe_2O_3	4.36	1.86	1.97	2.07	1.56	1.08	2.18
MnO	0.01	0.02	0.02	0.02	0.02	0.03	0.02
MgO	2.85	1.51	1.55	1.56	1.31	1.03	1.29
CaO	20.40	42.7	42.4	42.3	45.8	50.90	44.90
Na_2O	0.15	0.18	0.12	0.11	0.10	0.12	0.09
K_2O	3.70	1.40	1.36	1.33	0.87	0.32	0.92
P_2O_5	n.d.	0.01	0.02	0.02	0.04	0.09	0.05
LOI	24.10	36.44	36.51	36.57	39.12	42.34	39.15
ppm							
Rb	170	54	54	53	37	9	33
Ba	218	87	110	114	79	34	58
Sr	128	147	165	168	178	183	157
Th	8	10	11	10	10	9	7
Hf	3	2	2	2	1	0.3	1
Ta	1	1	1	1	0.4	0.1	0.3
Co	6	3	4	5	4	2	1
Sc	11	7	7	7	6	4	5
V	212	67	71	74	53	30	72
Cr	96	38	42	43	33	11	23
Cs	11	4	4	4	3	1	3
Ni	83	43	46	48	35	21	33
Y	6	5	11	9	8	8	6
Zr	107	63	83	73	37	12	32
Nb	8	6	6	4	2	n.d.	n.d.
La	13	21	26	24	26	23	17
Ce	33	40	53	52	55	47	34
Nd	n.d.	18	24	25	24	23	17
Sm	3	4	5	5	6	6	4
Eu	0.4	1	1	1	1	1	1
Tb	0.3	0.5	0.6	0.6	1	1	0.4
Yb	1	2	1.6	1.6	1	1	1
Lu	0.2	0.2	0.3	0.2	0.2	0.2	0.2
ΣREE	50.9	86.7	111.5	109.4	114.2	102.2	74.6

kaolinite and minor anatase (Mongelli, 1997; Mongelli and Acquafredda, 1999), and their origin was related to alteration of pyroclastics with minor contributions from the residuum of platform limestone. This mixing model is based on Sm/Nd and Eu/Eu* ratios, which should have remained unchanged during bauxitization, and is consistent with the tectonic regime of the Tethyan area in the Late Cretaceous (D'Argenio and Mindszenty, 1995).

The lack of observed volcanic shards in the BR bed precludes such a contribution to its formation. Thus, comparing the composition of this Turonian sediment derived from the dissolution of the ACP only with a coeval sediment possibly derived from both carbonate residuum and pyroclastics, may furnish

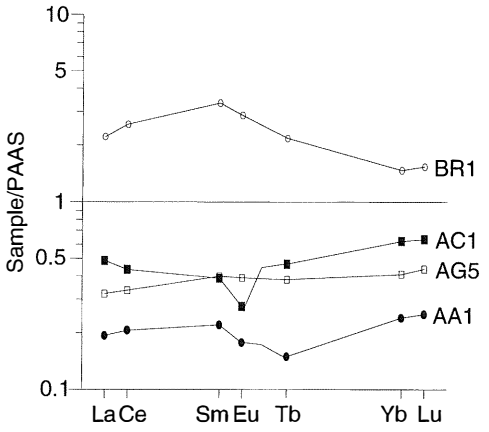

Fig. 6 – REE patterns of four selected samples normalized to the PAAS. See text for discussion.

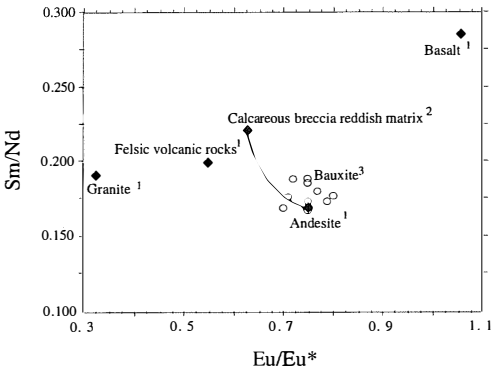

Fig. 7 – Eu/Eu* *vs* Sm/Nd diagram. Data sources: 1) Condie (1993); 2) this study; 3) Comunale and Mongelli (submitted). See text for discussion.

additional information on the validity of the mixing model proposed for the Apulian bauxites. The reddish matrix of sample BRl has an Sm/Nd ratio higher than the Apulian karst bauxites (fig. 7). It also has a larger negative Eu-anomaly than the bauxites which have both Sm/Nd and Eu/Eu* ratios similar to that of volcanic rocks of intermediate composition. Although more data concerning REE distribution in the reddish matrix of the BR bed are needed, it appears that derivation of Apulian bauxite from both intermediate in composition pyroclastics and minor limestone residuum is consistent with these limited data.

Illite-rich beds (samples AG and AA)

The abundance of illite in marine sediments may derive from: illitization in the marine environment during burial and/or from terrigeneous supply. The sedimentological features support the formation of the Late Cretaceous succession of the ACP in shallow seawater without burial (e.g., Carannante, *et al.*, 1997). Therefore, illite was probably supplied by terrigeneous sources during cold to temperate climates, which favoured mainly direct rock erosion, as demonstrated by the abundance of detrital calcite in the studied rocks. Chemical fractionation and mineralogical changes were probably small, in agreement with both the observed alteration chemical index as defined by Nesbitt and Young (1984) reported in Table 7, and the low contents of expandable layers in the illite lattice. In addition, the mineralogical and chemical changes of detrital illite in sea water were probably minor (e.g., Hoffman, 1979). Therefore, the composition of these beds may reflect that of the platform limestone residue, and in fact is very similar to the composition of residue from the experimental dissolution of ACP material (Moresi and Mongelli, 1988). Both bulk rock beds and grain-size fractions show quite similar mineralogy and chemistry, suggesting that the depositional environment and residue composition remained unchanged from Turonian to Coniacian.

CONCLUSIONS

The marine clay-rich beds of Upper Cretaceous age interlayered with limestone in the ACP (samples AG and AA) probably represent the insoluble residue of an exposed eroded portion of the carbonate platform. In Cretaceous times, the ACP was sheltered from terrigeneous supply by deep troughs, and thus the insoluble residue must be related mostly to wind-borne dust incorporated in the limestone during platform accretion. The residue is illite-rich, in agreement with the worldwide observed high amounts of illite in Late Cretaceous rocks,

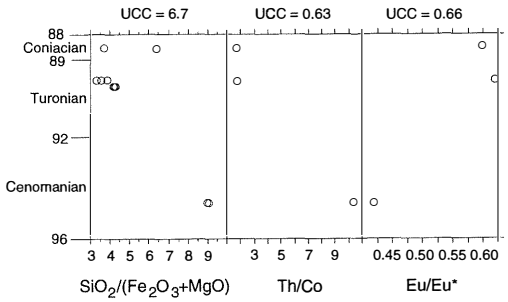

Fig. 8 – Elemental ratios of clay beds from ACP. A decrease of «felsic» character of beds during time would seem to be occurred. See text for discussion.

this mineral being related to continental wind-borne dust (Chamley, 1989). The siliciclastic component of the Turonian and Coniacian pelitic beds is very similar in composition to the insoluble residue obtained from acid dissolution of ACP limestone. This suggests, consistent with the values of the chemical index of alteration that the original composition of wind-borne dust was basically preserved in the beds.

The smectite-rich Cenomanian bed (samples AC) appears to have formed from more evolved material, the peculiar features of which may have been acquired either prior to incorporation in ACP limestone or during carbonate weathering. The precursor was probably represented by wind-borne dust with comparatively higher Th/Co and $SiO_2/(Fe_2O_3+MgO)$ and lower Eu/Eu* ratios (fig. 8) with respect to the illite-rich beds. Explanations may be that wind-borne dust derived from: 1) various continental areas; 2) a given continental area when it originated in different climates, or 3) the same continental areas, with the same climate, but coarser and heavier dust particles were transported by more energetic winds after the Cenomanian.

The kaolinite-rich Turonian bed (samples BR) formed in a warm, humid climate via platform limestone dissolution and accumulation on land. It is coeval with ACP karst bauxite. The Eu/Eu* and Sm/Nd ratios support a binary origin of bauxite from intermediate pyroclastics and limestone residue. This model is consistent with the occurrence of large-scale tectonic movements, including subduction and continental collision of the northern margin of the Adria plate (e.g., D'Argenio and Mindszenty, 1986), which gave rise to volcanic activity in the Tethyan area during the Late Cretaceous.

ACKNOWLEDGEMENTS

This paper benefited significantly from comprehensive reviews by Professor G. Cortecci and an anonymous reviewer, to whom we extend our heart felt thanks.

REFERENCES

ANDREOZZI M., DINELLI E. and TATEO F. (1997) — *Geochemical and mineralogical criteria for the identification of ash layers in the stratigraphic framework of a foredeep; the Early Miocene Mt. Cervarola Sandstones, northern Italy*. Chem. Geol., **137**, 29-39.

BISCAYE P.E. (1965) — *Mineralogy and sedimentation of recent deep-sea clay in the Atlantic Ocean adjacent seas and oceans*. Geol. Soc. Am. Bull., **76**, 803-832.

BONNOT-COURTOIS C. (1981) — *Géochimie des terres rares dans le principaux milieux de formation et de sédimentation des argiles*. Thèse, Sci. Nat., Paris-Sud, 230 pp.

CARANNANTE G., GRAZIANO R., RUBERTI D. and SIMONE L. (1997) — *Upper Cretaceous temperate-type shelves from Northern (Sardinia) and Southern (Apennines-Apulia) Mesozoic Tethyan margins*. In: N.P. James and J.A.D. Clarke (Editors) - *Cool-water carbonates*. SEPM, Tulsa, 309-325.

CHAMLEY H. (1989) — *Clay sedimentology*. Springer-Verlag, Berlin, 623 pp.

COMUNALE G. and MONGELLI G. (submitted) — *Are karst bauxites the weathering product of a carbonate protolith? The case of the Late Cretaceous bauxites from the Apulia carbonate platform, southern Italy*. Per. Mineral.

CONDIE K.C. (1993) — *Chemical composition and evolution of the upper continental crust: contrasting results from surface samples and shales*. Chem. Geol., **104**, 1-37.

D'ARGENIO B. and MINDSZENTY A. (1986) — *Cretaceous bauxites in the tectonic framework of*

the Periadriatic Region. Rend. Soc. Geol. It., **9**, 257-262.

D'ARGENIO B. and MINDSZENTY A. (1995) — *Bauxites and related paleokarst: tectonic and climatic event markers at regional unconformities.* Eclogae geol. Helv., **88/3**, 453-499.

D'ARGENIO B., MINDSZENTY A., BARDOSSY G., JUHASZ E. and BONI M. (1986) - *Bauxites of southern Italy revisited.* Rend. Soc. Geol. It., **9**, 263-268.

DOGLIONI C. and FLORES G. (1994) — *An introduction to Italian geology.* Editrice Il Salice, 91 p.

EBERLI G.P. (1991) — *Growth and demise of isolated carbonate platforms – Bahamian controversies.* In: D.W. Müller, J.A. McKenzie and H. Weissert (Editors) - *Controversies in Modern Geology.* Academic Press, London, 231-248.

EBERLI G.P., BERNOULLI D., SANDERS D. and VECSEI A. (1993) — *From aggradation to progradation: the Maiella Platform, Abruzzi, Italy.* In: J.A. Toni Simo, R.W. Scott and J.P. Masse (Editors) - *Cretaceous Carbonate Platforms.* AAPG Memoir, **56**, Tulsa, 213-232.

FERRERI V., WEISSERT H., D'ARGENIO B. and BUONOCUNTO F.P. (1997) - *Carbon isotope stratigraphy: a tool for basin to carbonate platform correlation.* Terra Nova, **9**, 57-61.

FRANZINI M., LEONI L. and SAITTA M. (1972) — *A simple method to evaluate the matrix effects in X-ray fluorescence analysis.* X-ray Spectrom., **1**, 151-154.

FRANZINI M., LEONI L. and SAITTA M. (1975) — *Revisione di una metodologia analitica per fluorescenza X basata sulla correzione completa degli effetti di matrice.* Soc. Ital. Mineral. Petrol., **31**, 365-378.

GORDON G.E., RANDLE K., GOLES G., CORLISS J., BEESON M.H. and OLSEY S.S. (1968) — *Instrumental neutron activation analysis of standard rocks with high resolution gamma-ray detectors.* Geochim. Cosmochim. Acta, **32**, 369-396.

HAQ B.U., HARDENBOL J. and VALE P. (1988) — *Mesozoic and Cenozoic chronostratigraphy and cycles of sea-level change.* In: C.K. Wilgus, C.G.St.C. Kendall, H.W. Posamentier, C.A. Ross and J.C. Van Wagoner (Editors) - *Sea level changes – an integrated approach.* SEPM Special Pubblication, **42**, Tulsa, 71-108.

HOFFMAN J.C. (1979) — *An evaluation of potassium uptake by Mississippi river borne clays following deposition in the Gulf of Mexico.* Ph. D. Diss., Case Western Reserve Univ., Cleveland, Ohio.

IANNONE A. and LAVIANO A. (1980) — *Studio stratigrafico e paleoambientale di una successione Cenomaniano-Turoniana (Calcare di Bari) affiorante presso Ruvo di Puglia.* Geol. Rom., **19**, 209-230.

JACOBS J.W., KOROTOV R.L., BLANCHARD D.P. and HASKINS L.A. (1977) — *A well tested procedure for instrumental neutron activation analysis of silicate rocks and minerals.* J. Radioanalyt. Chem., **40**, 93-114.

JENKYNS H.C. (1988) — *The Early Toarcian (Jurassic) anoxic event: stratigraphic, sedimentary, and geochemical evidence.* Am. J. Sci., **288**, 101-151.

JENKYNS H.C. (1995) — *Carbon-isotope stratigraphy and paleoceanographic significance of the lower Cretaceous shallow-water carbonates of Resolutio Guyot, Mid-Pacific Mountains.* Proc. Ocean Drill. Progr. Sci. Res., **143**, 99-104.

LAVIANO R. (1987) — *Analisi mineralogica quantitativa di argille mediante diffrattometria di raggi X.* Collana di studi ambientali. Procedure di analisi di minerali argillosi, Ente Nazionale Energie Alternative, 215-234.

LAVIANO R. and MONGELLI G. (1996) — *Geochemistry and mineralogy as indicators of parental affinity for Cenozoic bentonites: a case study from S. Croce di Magliano (southern Apennines, Italy).* Clay Min., **31**, 391-401.

LAVIANO A., GALLO MARESCA M. and TROPEANO M. (1998) — *Stratigraphic organization of rudist biogenic beds in the Upper Cenomanian successions of the western Murge (Apulia, Italy).* Geobios, Mém. sp., **22**, 159-168.

LEONI L. and SAITTA M. (1976) — *Determination of yttrium and niobium on standard silicate rocks by X-ray fluorescence analysis.* X-ray Spectrom., **5**, 29-30.

LUPERTO SINNI E. (1996) — *Sintesi delle conoscenze biostratigrafiche del Cretaceo del Gargano e delle Murge.* Mem. Soc. Geol. It., **51**, 995-1018.

LUPERTO SINNI E. and REINA A. (1996) — *Gli hiatus del Cretaceo delle Murge: confronto con dati offshore.* Mem. Soc. Geol. It., **51**, 719-727.

MONGELLI G., CULLERS R.L. and MUELHEISEN S. (1996) — *Geochemistry of late Cretaceous-Oligocenic shales from the Varicolori Formation, southern Apennines, Italy: implications for mineralogical, grain-size control and provenance.* Eur. J. Mineral., **8**, 733-754.

MONGELLI G. (1997) — *Ce-anomalies in the textural components of Upper Cretaceous karst bauxites from the Apulian carbonate platform, southern Italy.* Chem. Geol., **140**, 69-79.

MONGELLI G. and ACQUAFREDDA P. (1999) — *Ferruginous concretions in a Late Cretaceous karst bauxite: composition and conditions of formation.* Chem. Geol., **158**, 315-320.

MORESI M. and MONGELLI G. (1988) — *The relation between the terra rossa and the carbonate-free residue of the underlying limestones and dolostones in Apulia, Italy*. Clay Min., **23**, 439-446.

NESBITT H.W. and YOUNG G.M. (1984) — *Prediction of some weathering trends of plutonic and volcanic rocks based on thermodynamic and kinetic considerations*. Geochim. Cosmochim. Acta, **48**, 1523-

PLANCK T. and LANGMUIR C.H. (1998) — *The chemical composition of subduction sediment and its consequences for the crust and mantle*. Chem. Geol., **145**, 325-394.

PRICE G.D. (1999) – *The evidence and implications of polar ice during the Mesozoic*. Earth Sci. Rev., **48**, 183-210.

SCHLANGER W. (1981) — *The paradox of drowned reefs and carbonate platforms*. Geol. Soc. Amer. Bull., **92**, 197-211.

SHEPARD F.P. (1954) — *Nomenclature based on sand-silt-clay ratios*. J. Sedim. Petrol., **24**, 151-158.

SRODON J. (1980) — *Precise identification of illite/smectite interstratifications by X-ray powder diffraction*. Clay Min., **28**, 401-411.

TAYLOR S.R. and MCLENNAN S.M. (1985) — *The Continental Crust: its composition and evolution*. Blackwell, Oxford, 312 pp.

WEBER F., DUNOUER DE SEGONZAC G. and ECONOMOU C. (1976) — *Une nouvelle expression de la «Cristallinité» de l'illite et des micas. Notion d'epaisseur «apparente» des cristallites*. Compt. Rend. Somm. Soc. Geol. Fr., **5**, 225-227.

WRAY D.S. (1995) — *Origin of clay-rich beds in Turonian chalks from lower Saxony, Germany – a rare-earth element study*. Chem. Geol., **119**, 161-173.

ZHANG J. and NOZAKI Y. (1998) — *Behaviour of rare earth elements in seawater at the ocean margin: a study along the slopes of the Sagami and Nankai troughs near Japan*. Geochim. Cosmochim. Acta, **62**, 1307-1317.